Combined wet and dry cleaning of SiGe(001)

Sang Wook Park, Tobin Kaufman-Osborn, and Hyonwoong Kim
Materials Science and Engineering Program, University of California, San Diego, La Jolla, California 92093

Shariq Siddiqui and Bhagawan Sahu
TD Research, GLOBALFOUNDRIES USA, Inc., 257 Fuller Road, Albany, New York 12203

Naomi Yoshida and Adam Brandt
Applied Materials, Inc., Santa Clara, California 95054

Andrew C. Kummel[a)]
Department of Chemistry and Biochemistry, University of California, San Diego, La Jolla, California 92093

(Received 31 December 2014; accepted 19 May 2015; published 17 June 2015)

Combined wet and dry cleaning via hydrofluoric acid (HF) and atomic hydrogen on $Si_{0.6}Ge_{0.4}(001)$ surface was studied at the atomic level using ultrahigh vacuum scanning tunneling microscopy (STM), scanning tunneling spectroscopy (STS), and x-ray photoelectron spectroscopy to understand the chemical transformations of the surface. Aqueous HF removes native oxide, but residual carbon and oxygen are still observed on $Si_{0.6}Ge_{0.4}(001)$ due to hydrocarbon contamination from post HF exposure to ambient. The oxygen contamination can be eliminated by shielding the sample from ambient via covering the sample in the HF cleaning solution until the sample is introduced to the vacuum chamber or by transferring the sample in an inert environment; however, both processes still leave carbon contaminant. Dry *in-situ* atomic hydrogen cleaning above 330 °C removes the carbon contamination on the surface consistent with a thermally activated atomic hydrogen reaction with surface hydrocarbon. A postdeposition anneal at 550 °C induces formation of an atomically flat and ordered SiGe surface observed by STM. STS verifies that the wet and dry cleaned surface has an unpinned Fermi level with no states between the conduction and valence band edge comparable to sputter cleaned SiGe surfaces. © *2015 American Vacuum Society*.
[http://dx.doi.org/10.1116/1.4922282]

I. INTRODUCTION

In order to overcome challenges when scaling down silicon-based complementary metal-oxide semiconductor devices, SiGe has received much attention due to its high carrier mobility and application in strain engineering.[1–3] SiGe has a higher hole mobility, which makes it useful as a replacement for Si as a channel material in P-type metal-oxide-semiconductor (PMOS) transistors.[4–6] Additionally, the larger lattice constant of SiGe can be utilized to improve electron mobility in N-type metal-oxide-semiconductor transistors by inducing a biaxial tensile strain into Si channels.[7–12] However, integration of SiGe as a channel material requires a clean and well-ordered surface for gate oxide deposition.[13] As the thickness of gate oxide scales down for high performance and low power consumption, a high quality interface between the high-k metal oxide and SiGe determines the device performance characteristics such as leakage current, mobility, and interface trap density (D_{it}).[14,15]

Several cleaning procedures have been explored on SiGe surfaces. HCl solution cleaning is an ineffective method to remove native oxide because SiO_2 is inert to HCl solutions.[16] Hydrofluoric acid (HF) treatment removes all the surface oxides, leaving the surface hydrogen terminated after transfer to UHV as shown by synchrotron high resolution x-ray photoelectron spectroscopy (XPS); however, an inert processing environment is required to avoid oxygen and carbon contamination since the hydrogen passivated Si(001) and Ge(001) surfaces after HF cleaning are not stable in the ambient air.[17–19] It is expected that GeH_x species are less stable than SiH_x species in ambient due to their weaker bonds.[19–21] Supercritical CO_2 containing HF and H_2O removes all native oxides on SiGe surfaces; however, this method requires high HF concentrations resulting in rougher surfaces.[22]

The study seeks to understand the chemical transformations required to produce a clean and uniform SiGe(001) surface. A combined wet and dry cleaning procedure is employed to remove O and C, maximize the nucleation density of high-k atomic layer deposition, and prepare a good template for subsequent forming gas anneal.[23–25] XPS measurements show that two newly developed HF wet clean methods remove the SiGe oxides leaving the surface chemically passivated, thereby avoiding substrate oxidation even during ambient exposure. Even though ambient exposure results in hydrocarbon contamination, it is readily removed by subsequent atomic H exposure. The atomic H cleaning also induces Si segregation onto the surface while maintaining a good electronic structure. Si termination is likely to be advantageous for device performance due to the low defect density of Si/high-*k* dielectric interfaces after forming gas annealing.[26] Furthermore, Si termination on Ge PMOS transistors minimizes the interface trap density (D_{it}).[27] In the present study, each experimental step is verified using *in-situ* XPS, scanning tunneling microscopy (STM), and scanning tunneling spectroscopy (STS).

[a)]Electronic mail: akummel@ucsd.edu

II. EXPERIMENT

N-type $Si_{0.6}Ge_{0.4}(001)$ layers with 4×10^{19} cm^{-3} P doping grown on Si(001) were prepared by Applied Materials and diced into 12×4.5 mm pieces. Samples were degreased with acetone, methanol, and deionized water using ultrasonication three times then dried with N_2 gas.

Samples were dipped into 2% HF solution for 2 min to remove native oxide and loaded within 5 min into a custom Omicron UHV chamber with a base pressure of 2×10^{-10}. Samples were annealed at 100, 200, and 500 °C via direct heating. The sample temperatures were monitored by a pyrometer and heated at a rate of 1 °C/s. Chemical, topological, and electronic properties were verified via XPS, STM, and STS in each experiment.

Two methods, "toluene double dip" and "HF drop," were investigated to eliminate residual oxygen on the surface. It was hypothesized that residual oxygen on the surface came from ambient hydrocarbon; therefore, deposition of a clean hydrocarbon capping layer was investigated. For the toluene double dip method, toluene was layered onto 2% HF solution to coat the SiGe upon removal from the HF solution; to insure no residual HF, after the samples were pulled out of the solution, samples were transferred to another toluene solution. SiGe surfaces remained covered with a layer of toluene to minimize air exposure during the transfer. In HF drop, after the normal HF clean without toluene, an additional 2% HF solution was dropped onto samples in the load lock under N_2 purge and evaporated in the load lock chamber during pump down to a base pressure of 2×10^{-8} Torr. After each cleaning method, the samples were annealed at 150 and 300 °C via resistive PBN heating; the surface composition after each step was determined by *in-situ* XPS.

After the drop clean method, SiGe samples were exposed to atomic hydrogen in the UHV chamber using a thermal gas cracker (Atomic Hydrogen Source, Veeco). The gas pressure was controlled via a leak valve and measured through an ion gauge; the exposure was calculated in terms of Langmuirs [1 Langmuir (L) $= 1 \times 10^{-6}$ Torr 1 s]. During the gas dosing, the filament temperature of thermal gas cracker was 1800–2200 °C while SiGe(001) samples were maintained at 330 °C using a resistive PBN heater. The exposure pressures were measured with an ion gauge and calculated in Langmuirs; therefore, the reported doses are based on the H_2 pressure and are an upper limit to the true exposure. The cracking efficiency is expected to be 30% (Veeco), but it could not be verified.

Samples were transferred to a STM chamber with a base pressure of 1×10^{-11} Torr. The atomic and electronic structures of SiGe surface in each experiment were studied with *in-situ* STM and STS at 300 K (LT-STM, Omicron Nanotechnology). Constant-current STM ($I_{sp} = 200$ pA) was operated with a sample bias between −1.8 and −2.0 V to obtain filled state STM images. Variable-z mode STS was operated using a modulation signal (0.1 V, 650 Hz) from an external lock-in amplifier (SR830 DSP, Stanford Research Systems) while sweeping the sample bias from −1.5 to +1.5 V.

Chemical analysis was performed using an *in-situ* monochromatic XPS (XM 1000 MkII/SPHERA, Omicron Nanotechnology). Constant analyzer energy mode with a pass energy of 50 eV and a line width of 0.1 eV using an Al Kα source (1486.7 eV) were employed. The takeoff angle was 30° from the sample surface, which is close to surface parallel, and an acceptance angle of ±7° was employed. For peak shape analysis, CASA XPS v.2.3 was employed using a Shirley background subtraction.

III. RESULTS AND DISCUSSION

A. Wet cleaning

$Si_{0.6}Ge_{0.4}(001)$ surfaces were cleaned via a 2% HF solution method leaving the surface hydrogen terminated at room temperature as reported in a previous study using synchrotron radiation photoelectron spectroscopy.[16] Figure 1(a) shows XPS results of SiGe(001) surface after 100, 200, and 500 °C anneals. All XPS peaks are normalized by photoelectron cross-sections (Si2p-0.817, Ge 3d-1.42, O 1s-2.93, C 1s-1) using Hartree–Slater atomic model.[28] Moreover, it is assumed that elements such as oxygen and carbon are present as adsorbates on the SiGe(001) substrate. Since the escape depth of electrons from the Si2p and Ge3d peak is approximately 1 nm for a detection angle of 30° from the sample surface based on a model by Seah and Dench,[29] for the 44% in the C/(Si + Ge) and 14% in the O/(Si + Ge) ratios shown in Fig. 1, the real surface concentrations correspond to approximately 2.3

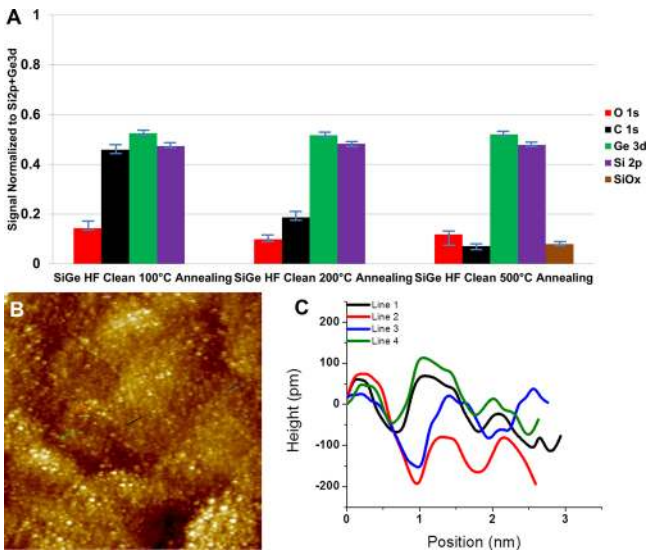

FIG. 1. (Color online) XPS and STM of wet cleaned SiGe(001). (a) XPS data of HF wet cleaned SiGe(001) surface followed by annealing at 100, 200, and 500 °C. The ratio of each chemical element is normalized to the sum of all components of Si 2p and Ge 3d peaks. (b) Filled state STM image (50×50 nm^2, $V_s = -1.8$ V, and $I_t = 200$ pA) of wet cleaned and 500 °C annealed SiGe(001). (c) Line trace analysis of four different areas on STM image (left). Vertical order is shown and average of row spacing is 1.2 nm with a standard error of 0.055 nm.

ML carbon and 0.7 ML oxygen. These numerical values are obtained based on a simplified model in which the top three monolayers are purely composed of C and O atoms and the lower layers are composed of Si and Ge atoms and the attenuation is estimated using the formula $I = I_o\exp(-t/\lambda)$ (I: intensity in the presence of the overlayer, I_o: intensity in the absence of any covering layer, t: thickness of the layer, λ: inelastic mean free path). The presence of oxygen is likely due to Si because Si-O bonds are stronger than Ge-O bonds and because H terminated Ge(001) exhibits only carbon contamination in ambient as shown by Rivillon *et al.*[19] Moreover, as shown by Hirose *et al.*, Si(001) rapidly absorbs a submonolayer of oxygen in ambient due to defects and weakly bound hydrides consistent with Si in SiGe(001) being responsible for oxygen contamination.[21] It is expected that the H termination is desorbed for the 500 °C anneal as shown in previous reports.[16,30] In the absence of strong adsorbate bonding, the surface of SiGe(001) is terminated by Ge atoms due to the segregation of Ge to the surface as reported in the previous studies.[31–33] Density functional theory calculations theoretically verified that clean SiGe(001) surfaces are thermodynamically more stable when composed of Ge atoms compared to Si atoms.[34] The wet cleaned surface of SiGe(001) shows a high percentage of Ge atoms because the native oxide of SiGe is mainly composed of SiO_2, and the SiO_2 is removed by wet HF thereby exposing the accumulation of Ge underneath the native oxide as reported in the previous report.[35] Since the Si/Ge ratio is identical on all surfaces independent of annealing condition (Fig. 1), it is concluded that the wet cleaned surfaces are largely Ge enriched.

XPS data show that wet HF cleaned SiGe surfaces contain residual oxygen and carbon. Since no SiO_x nor GeO_x components are present, the XPS data are consistent with the C and O being in the form of hydrocarbon due to air exposure during the transfer into the load lock. The surface concentration of carbon and oxygen decreases upon heating to 200 °C. However, as the temperature is increased up to 500 °C, the O is transferred to Si atoms forming surface SiO_x before the hydrocarbon completely desorbs while in UHV adsorbate-free annealed SiGe(001), Ge is terminated.[34] In the previous study, it is reported that "reverse segregation" at the surface is induced between Si and Ge by atomic hydrogen exposure because the Si-H bond is much stronger than Ge-H bond.[36,37] A similar phenomenon of reverse segregation should be expected on the SiGe(001) surface if there is a full monolayer of oxygen because the Si-O bond is much stronger than the Ge-O bond.

Figure 1(b) shows a filled-state STM image of a SiGe(001) surface after a 500 °C anneal. The STM image shows that HF wet clean and 500 °C anneal result in a surface with a root mean square (RMS) roughness of 0.40 nm. Since the wet clean surface contains only small domains and a high concentration of surface contaminants, a line trace analysis is needed to accurately determine the surface atomic space. To determine the vertical row spacing of HF wet cleaned and annealed SiGe(001) surface, line traces of four different areas are analyzed in Fig. 1(c). Line trace analysis shows an average row spacing of 1.2 nm with a standard error (SE) of 0.055 nm consistent with the row spacing of the ideal SiGe(001) surface.

B. Toluene double dip

In the present study, two methods of enhanced wet cleaning, toluene double dip and HF drop, were investigated to eliminate residual oxygen on the SiGe(001) surface. Since residual oxygen mainly results from the air exposure during the sample transfer, each method was designed to protect the surface against oxidation by oxy-hydrocarbons from air by covering the surface with a hydrophobic toluene layer or using an N_2 purge. Figure 2(a) shows the schematic of the toluene double dip method. It was hypothesized that if toluene sticks to the residual reactive sites on the HF wet cleaned sample, this would inhibit adsorption of oxy-hydrocarbons. Toluene is a hydrophobic molecule with strong internal bonds, which should adsorb onto hydrogen terminated SiGe(001) surface without any chemical reaction and easily evaporate in a vacuum chamber due to its high vapor pressure at RT. XPS data show that toluene double dip results in no oxygen and low carbon contamination in Fig. 2(b). As the sample temperature was increased to 300 °C, toluene capped SiGe(001) surface had only 4% oxygen, which is 50% smaller than normal HF cleaned SiGe(001). The residual oxygen is probably due to contamination from the vacuum system since it was not present on the sample prior to annealing.

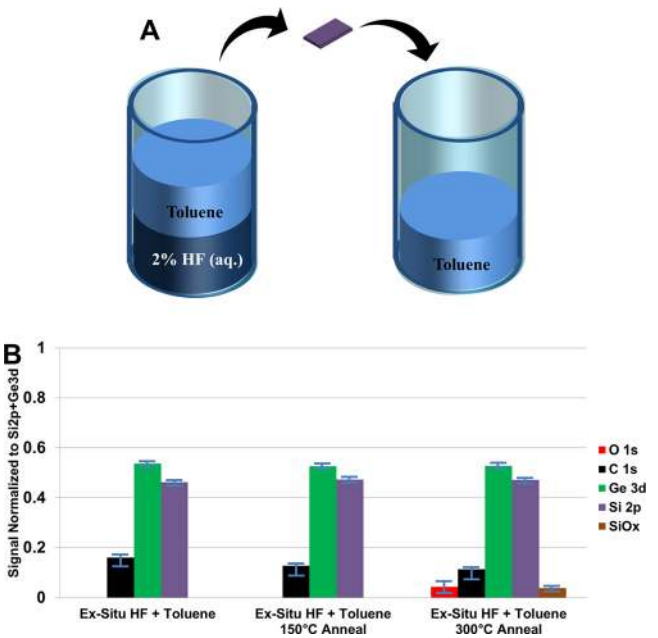

FIG. 2. (Color online) Schematic image and XPS of toluene double dip method. (a) Schematic diagram of toluene double dip method. Wet HF cleaned SiGe(001) samples are pulled through a layer of toluene then dipped into another toluene solution. (b) XPS data of toluene double dip method followed by 150 and 300 °C anneal.

C. Wet and dry cleaning

For the HF drop method, after HF wet clean, additional HF solution is dropped onto SiGe(001) surface in the load lock under N_2 purge, which is known to stabilize Ge-H bonds in ambient.[19] The HF is evaporated in a vacuum chamber during evacuation via a turbo pump. As shown in Fig. 3(a), after the HF drop clean, the SiGe(001) surface contains no oxygen, but still contains carbon comparable to *ex-situ* HF clean.

To remove the carbon from the HF drop cleaned SiGe(001) surface, atomic hydrogen was employed while the substrate temperature was maintained at 330 °C. In the previous studies, atomic hydrogen cleaning at temperatures higher than 250 °C prevented preferential etching of Ge due to inhibition of GeH_2 formation at elevated temperature[38,39] and atomic hydrogen cleaning is known to induce a Si segregation on Ge-covered Si(001) by suppressing Ge segregation above the substrate temperature of 250 °C.[37] Additionally, it was reported that atomic hydrogen suppresses the Ge surface segregation during molecular beam epitaxy growth of Si/Ge heterostructures.[40] It is anticipated that similar phenomena should be observed on SiGe(001) when dosed with atomic hydrogen at 330 °C. The SiGe(001) surface was dosed with 18 000 L of atomic hydrogen while the substrate temperature was maintained at 330 °C. XPS results in Fig. 3(a) show that

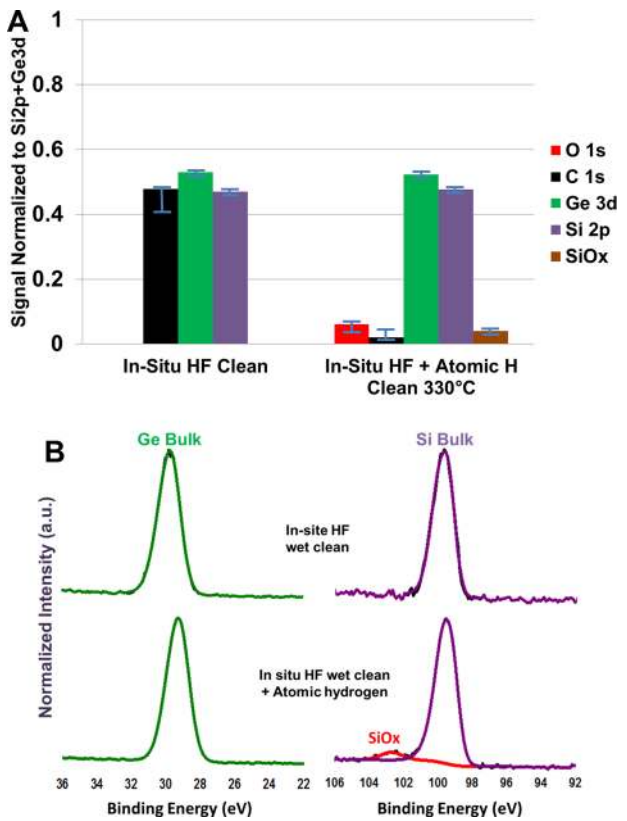

FIG. 3. (Color online) XPS analysis of wet plus dry cleaned SiGe(001). (a) XPS data of HF drop method followed by 18 000 L atomic H clean shows atomic H removes carbon from SiGe(001) surface. (b) XPS analysis before and after atomic H clean show the change of spectrum in Ge 3d and Si 2p peaks shows the absence of any initial Si and Ge oxides and only 6% SiO_x due to oxygen contamination during the atomic H clean.

almost all carbon is eliminated, but 6% of oxygen is introduced because the high temperature of tungsten filament of thermal gas cracker induces wall desorption of oxygen in the UHV chamber, which forms SiO_x on Si-enriched SiGe(001) surfaces. Figure 3(b) shows the spectrum of Ge 3d and Si 2p peak after the wet HF drop method and dry atomic H clean. Si 2p peak shows the formation of shoulder at higher binding energy corresponding to SiO_x after atomic H clean whereas Ge 3d peak shows no changes. This is consistent with the atomic H clean inducing or maintaining a Si enriched SiGe(001) surface.

Figure 4 shows STM images of HF drop cleaned SiGe(001) after atomic H cleaning at 330 °C and subsequent anneals at 330 and 550 °C. Due to the small domain size and residual oxygen contamination, line trace analysis is needed to quantitatively determine the surface order. The SiGe(001) surfaces with only 330 °C anneal [Fig. 4(a)] have a RMS roughness of 0.29 nm and an average row spacing of 1.2 ± 0.049 nm (SE) as shown in Fig. 4(c); this is the identical row spacing as the sputter cleaned surface and, therefore, consistent with the ideal row spacing of SiGe(001) despite the small domain size and the residual surface contamination. Post clean annealing at 550 °C decreases the RMS roughness from 0.29 to 0.23 nm while maintaining 1.2 ± 0.044 nm (SE) row spacing as shown in Fig. 4(d); in addition, the STM images show no etch pits. Compared to the HF wet cleaned surface, combined wet and dry cleaning results in a flatter and more uniform surface as shown by the 30% decrease in RMS roughness and the appearance of distinct rows with the spacing of the ideal sputter-cleaned surface. Lower RMS roughness and the absence of etch pits are considered critical to high channel mobility.[41–44]

STS measurements were taken to determine the effect of the cleaning processes on the electronic structure of n-type SiGe(001) surfaces. Pinning of $Si_{0.6}Ge_{0.4}(001)$ results in a Fermi level near the valence band similar to Ge(001) so STS of n-type is sufficient to determine the unpinning of the surface.[45] STS measures the local density of states (LDOS) by lock-in measurement of the AC signal from AC modulation of the sample bias during an I-V (current–voltage) sweep of the DC sample bias to obtain (dI/dV)/(I/V), which is considered to be proportional to the LDOS.[46,47] STS curves in Fig. 5 show the HF drop cleaned surface after both atomic H cleaning and annealing at 550 °C produces an unpinned surface with same electronic structure (HF Drop+Dry Atomic H Clean) as sputter cleaned surface (Sputter Clean). Moreover, no states are detected in the band gap region between conduction and valence band edges in contrast to normal HF cleaned surface with band gap states (Normal HF Clean). This result demonstrates that a clean and unpinned SiGe surface is obtained through combined wet HF and dry atomic H cleaning method without sputter clean.

IV. SUMMARY AND CONCLUSIONS

HF wet clean was utilized to remove the native oxide of $Si_{0.6}Ge_{0.4}(001)$ surface; however, normal *ex-situ* HF wet

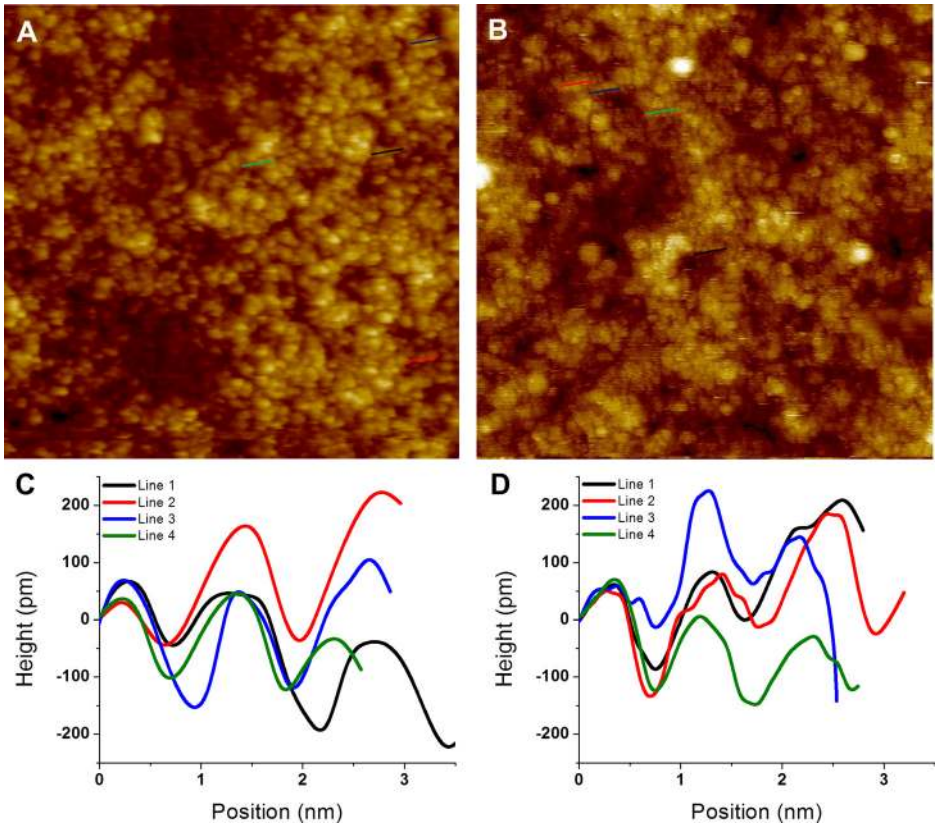

FIG. 4. (Color online) STM images of wet and dry cleaned SiGe(001). (a) Filled state STM image ($50 \times 50\,nm^2$, $V_s = -1.8$ V, $I_t = 200$ pA) after 330 °C anneal. (b) STM image ($50 \times 50\,nm^2$, $V_s = -1.8$ V, $I_t = 200$ pA) after 550 °C anneal. (c) Line traces of four different areas on STM image of SiGe(001) after 330 °C anneal (a) and average of row spacing is 1.2 nm with a standard error of 0.049 nm. (d) Line traces of four different areas on STM image of SiGe(001) after 550 °C anneal (b) and average of row spacing is 1.2 nm with a standard error of 0.043 nm.

cleaned SiGe(001) contains residual oxygen as a form of hydrocarbon. Two methods, toluene double dip and HF drop, were studied to eliminate residual oxygen. Toluene protects the surface against ambient deposition of oxy-hydrocarbon by toluene passivating the reactive SiGe surface defects. Since toluene has strong internal bonds, a high vapor pressure, and is hydrophobic, it leaves no significant dissociative chemisorption products on hydrogen terminated SiGe(001) surface and it prevents water condensation. The HF drop simulates HF clean with N_2 purge to minimize oxygen adsorption from ambient condition. HF drop clean eliminates oxygen from the SiGe(001) surface. In order to remove residual carbon, dry atomic hydrogen clean was investigated. The thermal atomic H clean at 330 °C both removed residual carbon and formed a Si enriched SiGe(001) surface consistently with only SiO_x and no GeO_x forming post H clean upon oxygen exposure. STS verified combined wet and dry clean provides the same electronic structures as sputter cleaned SiGe(001).

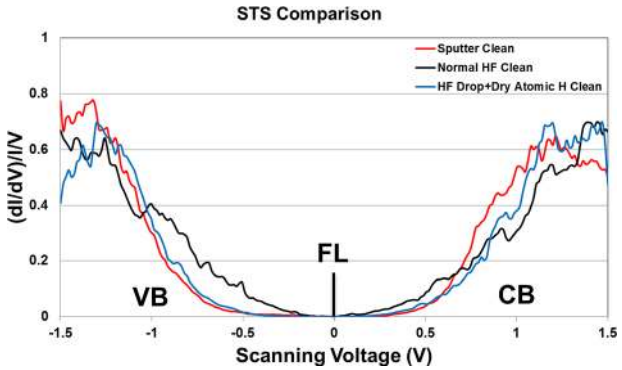

FIG. 5. (Color online) STS measurements of wet and dry cleaned SiGe(001). Combined HF drop and dry atomic H clean (HF Drop+Dry Atomic H Clean) shows no bandgap states compared to normal HF clean (Normal HF Clean) and results in identical LDOS as sputter cleaned SiGe(001) surface (Sputter Clean).

ACKNOWLEDGMENTS

This work was supported by the Semiconductor Research Corporation (Task 2451.001), NSF DMR 1207213, and Applied Materials. The SiGe wafers were provided by Applied Materials.

APPENDIX

To provide more accurate insight into experimental uncertainties, the raw XPS spectra of Ge 2p, Ge 3d, Si 2p were fitted to show the chemical shift with an error range of ±0.1 eV and the atomic ratios for the SiGe(001) surface are presented during the different cleaning methods. In addition, all XPS spectra are calibrated based on the C 1s

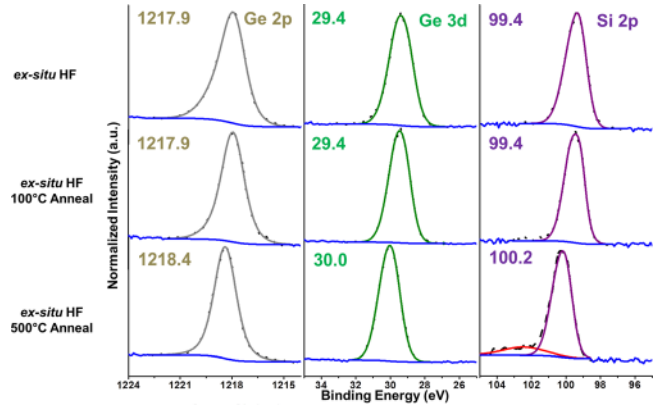

FIG. 6. (Color online) XPS spectra of Ge 2p, Ge 3d, and Si 2p on wet cleaned SiGe(001) followed by annealing. Annealing at 100 °C reduces the peak widths. Annealing at 500 °C induces the Ge peak to be symmetric but causes formation of a SiO_x peak. The numerical values in XPS spectra belong to peak positions.

peak at 284.5 eV and the chemical shifts of the Ge 2p peaks under all conditions are discussed due to its higher surface sensitivity and accuracy resulting from small escape depth and strong peak intensity compared to Ge 3d and Si 2p peaks.

As shown in Fig. 6, the XPS spectral peaks after HF wet clean are broad with the Ge 2p having FWHM of 1.81 eV compared to the sputter cleaned Ge 2p SiGe(001) surface with FWHM of 1.60 eV. This is mainly because the adsorbates such as carbon and oxygen cause small chemical shifts. After the annealing at 100 °C, the Ge 2p, Ge 3d, and Si 2p become sharper with a FWHM of 1.51 eV for Ge 2p consistent with desorption of hydrocarbons and other weakly bound contaminants. Even after the 500 °C annealing, the Ge 2p peak is at 1218.4 eV, which is shifted by 1.0 eV from the bulk value of 1217.4 eV on a sputter cleaned SiGe surface, consistent with desorption of hydrogen and bonding to remaining adsorbates. The energy shifts of the Ge 3d and Si 2p are not statistically significant due to the 10× lower signal to noise ratio and lower surface sensitivity of these peaks. The sensitivity corrected intensity ratios from Fig. 1(a) are provided in Table I.

XPS spectra after toluene double dip method are shown in Fig. 7. Compared to wet HF cleaned and 100 °C annealed SiGe(001), the nonannealed double dip clean surface contains low ratios of carbon and oxygen adsorbates as shown in Table II; the fraction of O is reduced from 0.14 to 0 and the fraction of C is reduced from 0.44 to 0.15 after toluene double dip method. The Ge 2p peak is at 1218.2 eV, which is shifted by 0.8 eV from the 1217.4 eV Ge 2p peak on a sputter cleaned SiGe surface, consistent with bonding to adsorbates and possibly some hydrogen. After 300 °C annealing, the Ge 2p peak still remains at the same position, indicating the surface is still terminated with hydrogen and adsorbates. The sensitivity corrected intensity ratios from Fig. 2(b) are provided in Table II.

TABLE I. Atomic ratios for wet cleaned SiGe(001) followed by annealing. All ratios are corrected by photoelectron cross-sections and normalized by Ge 3d + Si 2p peaks.

	Ex-situ HF + 100 °C anneal	*Ex-situ* HF + 200 °C anneal	*Ex-situ* HF + 500 °C anneal
O 1s	0.14 ± 0.03	0.10 ± 0.02	0.12 ± 0.04
C 1s	0.44 ± 0.03	0.18 ± 0.02	0.07 ± 0.02
Ge 3d	0.52 ± 0.01	0.51 ± 0.01	0.52 ± 0.01
Si 2p	0.48 ± 0.01	0.49 ± 0.01	0.48 ± 0.01
SiO_x	0.00	0.00	0.08 ± 0.01
Ge + Si	1.00	1.00	1.00

XPS spectra after wet and dry atomic H clean are shown in Fig. 8. The Ge 2p peak after *in-situ* wet clean is at 1218.3 eV, which is almost identical to 1218.2 eV on a toluene double dip cleaned SiGe surface, consistent with bonding primarily to the remaining adsorbates. The dry atomic H clean shifts the Ge 2p peak to 1217.7 eV, which is identical to the sputter cleaned surface after atomic H dose, consistent with all Ge surface atoms being Ge-H bonded. As shown in Table III, the fraction of C is reduced from 0.48 to 0.02 while the fraction of O is increased from 0 to 0.06 mainly due to adsorption of oxygen from operation of the high temperature atomic H source in the UHV chamber. The sensitivity corrected intensity ratios from Fig. 3(a) are provided in Table III.

XPS spectra after sputter and dry atomic H clean are shown in Fig. 9. The Ge 2p peak after sputter clean is at 1217.4 eV, which is lowest binding energy for any surface preparation condition, consistent with a clean surface without any hydrocarbon or hydrogen adsorbates at the surface as reported in the previous study.[48] After atomic H dose, the Ge 2p peak is shifted to higher binding energy by 0.3 eV from a sputter cleaned SiGe(001) surface mainly due to the hydrogen termination at the surface as shown in the previous study.[16] After 500 °C annealing, the Ge 2p peak is shifted back by 0.3–1217.4 eV binding energy since hydrogen atoms are desorbed and no adsorbates are present. Positions of peaks after each experimental step are compiled in Table IV.

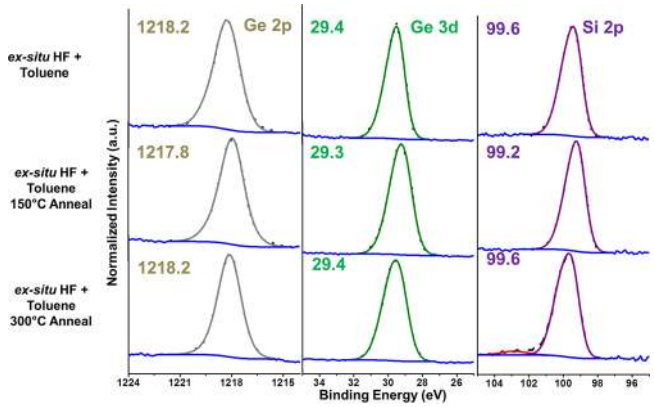

FIG. 7. (Color online) XPS spectra of Ge 2p, Ge 3d, and Si 2p of toluene double dip method followed by annealing. Annealing at 300 °C induces the Ge peak to be symmetric but causes formation of a SiO_x peak. The numerical values in XPS spectra belong to peak positions.

TABLE II. Atomic ratios for toluene double dip method followed by annealing. All ratios are corrected by photoelectron cross-sections and normalized by Ge 3d + Si 2p peaks.

	Ex-situ HF + toluene as-loaded	*Ex-situ* HF + toluene + 150 °C anneal	*Ex-situ* HF + toluene + 300 °C anneal
O 1s	0	0	0.04 ± 0.02
C 1s	0.15 ± 0.02	0.12 ± 0.02	0.11 ± 0.02
Ge 3d	0.53 ± 0.01	0.53 ± 0.01	0.53 ± 0.01
Si 2p	0.47 ± 0.01	0.47 ± 0.01	0.47 ± 0.01
SiO_x	0.00	0.00	0.03 ± 0.01
Ge + Si	1.00	1.00	1.00

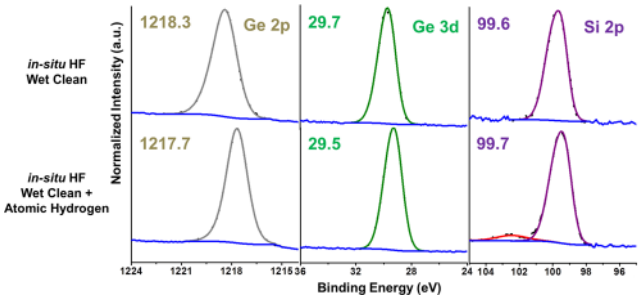

FIG. 8. (Color online) XPS spectra of Ge 2p, Ge 3d, and Si 2p of wet and dry clean followed by annealing. The atomic H causes the Ge peak to become symmetric but induces formation of a small SiO_x peak. The numerical values in XPS spectra belong to peak positions.

TABLE III. Atomic ratios for wet plus dry clean. All ratios are corrected by photoelectron cross-sections and normalized by Ge 3d + Si 2p peaks.

	In-situ HF as-loaded	*In-situ* HF + atomic hydrogen
O 1s	0.00	0.06 ± 0.02
C 1s	0.48 ± 0.05	0.02 ± 0.02
Ge 3d	0.53 ± 0.01	0.53 ± 0.01
Si 2p	0.47 ± 0.01	0.47 ± 0.01
SiO_x	0.00	0.04 ± 0.01
Ge + Si	1.00	1.00

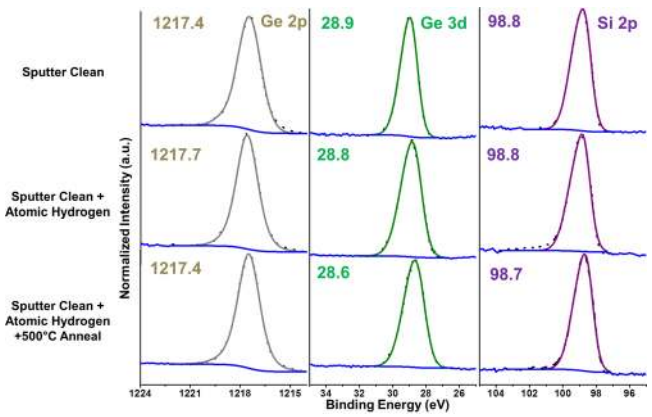

FIG. 9. (Color online) XPS spectra of Ge 2p, Ge 3d, and Si 2p of sputter and dry clean followed by annealing. The numerical values in XPS spectra belong to peak positions. The atomic H shifts the Ge 2p peak to higher binding energy and 500 °C anneal shifts the peak back to a lower binding energy consistent with the sputter cleaned position. The energy shifts of the Ge 3d and Si 2p are not statistically significant due to the 10× lower signal to noise ratio of these peaks.

TABLE IV. Positions of Ge 2p, Ge 3d, and Si 2p bulk peaks after each experimental step. Peak positions were calibrated based on the C 1s peak with an error range of ±0.1 eV. Ge 2p peak shifts under all conditions are significant due to their higher surface sensitivity and stronger peak intensities compared to Ge 3d and Si 2p peaks; the accuracies of the peak shifts for Ge 3d and Si 2p are close to ±0.3 eV due to the lower signal to noise ratios.

	Ex-situ HF wet clean as-loaded	*Ex-situ* HF wet clean + 100 °C anneal	*Ex-situ* HF wet clean + toluene as-loaded	*Ex-situ* HF wet clean + toluene + 150 °C anneal	*Ex-situ* HF wet clean + toluene + 300 °C anneal	*In-situ* HF wet clean as-loaded	*In-situ* HF wet clean + atomic H	Sputter clean as-loaded	Sputter clean + atomic H	Sputter clean + atomic H + 500 °C anneal
Ge 2p	1217.9	1217.9	1218.4	1217.8	1218.2	1218.3	1217.7	1217.4	1217.7	1217.4
Ge 3d	29.4	29.4	30.0	29.4	29.3	29.4	29.5	28.9	28.8	28.6
Si 2p	99.4	99.4	100.2	99.6	99.2	99.6	99.7	98.8	98.8	98.7

[1]F. Schaffler, Semicond. Sci. Technol. **12**, 1515 (1997).
[2]M. L. Lee, E. A. Fitzgerald, M. T. Bulsara, M. T. Currie, and A. Lochtefeld, J. Appl. Phys. **97**, 011101 (2005).
[3]D. J. Paul, Semicond. Sci. Technol. **19**, R75 (2004).
[4]T. Mizuno, N. Sugiyama, H. Satake, and S. Takagi, Symp. VLSI Technol., Dig. Tech. Pap. **2000**, 210.
[5]T. Mizuno, S. Takagi, N. Sugiyama, H. Satake, A. Kurobe, and A. Toriumi, IEEE Electron Device Lett. **21**, 230 (2000).
[6]M. L. Lee, C. W. Leitz, Z. Cheng, A. J. Pitera, T. Langdo, M. T. Currie, G. Taraschi, E. A. Fitzgerald, and D. A. Antoniadis, Appl. Phys. Lett. **79**, 3344 (2001).
[7]S. Datta *et al*., *Proceedings of the Bicmos Circuits and Technology Meeting* (IEEE, 2004), pp. 194–197.
[8]S. Datta *et al*., IEEE Int. Electron Devices Meet., Tech. Dig. **2003**, 653.
[9]N. Griffin, D. D. Arnone, D. J. Paul, M. Pepper, D. J. Robbins, A. C. Churchill, and J. M. Fernandez, J. Vac. Sci. Technol., B **16**, 1655 (1998).
[10]M. V. Fischetti, J. Appl. Phys. **89**, 1232 (2001).
[11]K. K. Rim, J. L. Hoyt, and J. F. Gibbons, IEEE Trans. Electron Devices **47**, 1406 (2000).
[12]S. H. Olsen, A. G. O'Neill, S. Chattopadhyay, L. S. Driscoll, K. S. K. Kwa, D. J. Norris, A. G. Cullis, and D. J. Paul, IEEE Trans. Electron Devices **51**, 1245 (2004).
[13]K. J. Kuhn, A. Murthy, R. Kotlyar, and M. Kuhn, ECS Trans. **33**, 3 (2010).
[14]K. Saraswat, C. O. Chui, T. Krishnamohan, D. Kim, A. Nayfeh, and A. Pethe, Mater. Sci. Eng., B **135**, 242 (2006).
[15]Y. Taur and T. H. Ning, *Fundamentals of Modern VLSI Devices*, 2nd ed. (Cambridge University, Cambridge; New York, 2009).
[16]Y. Sun, Z. Liu, S. Y. Sun, and P. Pianetta, J. Vac. Sci. Technol., A **26**, 1248 (2008).
[17]Y. J. Chabal, G. S. Higashi, K. Raghavachari, and V. A. Burrows, J. Vac. Sci. Technol., A **7**, 2104 (1989).
[18]X. Zhang, E. Garfunkel, Y. J. Chabal, S. B. Christman, and E. E. Chaban, Appl. Phys. Lett. **79**, 4051 (2001).
[19]S. Rivillon, Y. J. Chabal, F. Amy, and A. Kahn, Appl. Phys. Lett. **87**, 253101 (2005).
[20]E. Yablonovitch, D. L. Allara, C. C. Chang, T. Gmitter, and T. B. Bright, Phys. Rev. Lett. **57**, 249 (1986).
[21]F. Hirose, M. Nagato, Y. Kinoshita, S. Nagase, Y. Narita, and M. Suemitsu, Surf. Sci. **601**, 2302 (2007).
[22]B. Xie, G. Montano-Miranda, C. C. Finstad, and A. J. Muscat, Mater. Sci. Semicond. Process. **8**, 231 (2005).
[23]M. L. Reed and J. D. Plummer, J. Appl. Phys. **63**, 5776 (1988).
[24]K. L. Brower, Appl. Phys. Lett. **53**, 508 (1988).
[25]K. L. Brower, Phys. Rev. B **38**, 9657 (1988).
[26]M. Caymax, F. Leys, J. Mitard, K. Martens, L. J. Yang, G. Pourtois, W. Vandervorst, M. Meuris, and R. Loo, J. Electrochem. Soc. **156**, H979 (2009).
[27]M. Caymax, F. Leys, J. Mitard, K. Martens, L. J. Yang, G. Pourtois, W. Vandervorst, M. Meuris, and R. Loo, ECS Transactions **19**, 183 (2009).
[28]J. H. Scofield, J. Electron Spectrosc. **8**, 129 (1976).
[29]M. P. Seah and W. A. Dench, Surf. Interface Anal. **1**, 2 (1979).
[30]P. Gupta, V. L. Colvin, and S. M. George, Phys. Rev. B **37**, 8234 (1988).
[31]D. J. Godbey and M. G. Ancona, J. Vac. Sci. Technol., B **11**, 1392 (1993).
[32]D. J. Godbey and M. G. Ancona, Appl. Phys. Lett. **61**, 2217 (1992).
[33]G. G. Jernigan, P. E. Thompson, and C. L. Silvestre, Surf. Sci. **380**, 417 (1997).
[34]T. Kaufman-Osborn, E. A. Chagarov, S. W. Park, B. Sahu, S. Siddiqui, and A. C. Kummel, Surf. Sci. **630**, 273 (2014).
[35]H. K. Liou, P. Mei, U. Gennser, and E. S. Yang, Appl. Phys. Lett. **59**, 1200 (1991).
[36]Y. Kobayashi, K. Sumitomo, K. Shiraishi, T. Urisu, and T. Ogino, Surf. Sci. **436**, 9 (1999).
[37]E. Rudkevich, F. Liu, D. E. Savage, T. F. Kuech, L. McCaughan, and M. G. Lagally, Phys. Rev. Lett. **81**, 3467 (1998).
[38]Y. J. Zheng, P. F. Ma, and J. R. Engstrom, J. Appl. Phys. **90**, 3614 (2001).
[39]J. Y. Lee, S. J. Jung, J. Y. Maeng, Y. E. Cho, S. Kim, and S. K. Jo, Appl. Phys. Lett. **84**, 5028 (2004).
[40]G. Ohta, S. Fukatsu, Y. Ebuchi, T. Hattori, N. Usami, and Y. Shiraki, Appl. Phys. Lett. **65**, 2975 (1994).
[41]K. Sawano, K. Kawaguchi, T. Ueno, S. Koh, K. Nakagawa, and Y. Shiraki, Mater. Sci. Eng., B **89**, 406 (2002).
[42]T. Yamanaka, S. J. Fang, H. C. Lin, J. P. Snyder, and C. R. Helms, IEEE Electron Device Lett. **17**, 178 (1996).
[43]S. J. Fang, H. C. Lin, J. P. Snyder, C. R. Helms, and T. Yamanaka, Electrochem. Soc. **96**, 329 (1996).
[44]T. Ohmi, K. Kotani, A. Teramoto, and M. Miyashita, IEEE Electron Device Lett. **12**, 652 (1991).
[45]T. Kaufman-Osborn, E. A. Chagarov, and A. C. Kummel, J. Chem. Phys. **140**, 204708 (2014).
[46]R. M. Feenstra, Surf. Sci. **299–300**, 965 (1994).
[47]R. M. Feenstra, J. A. Stroscio, and A. P. Fein, Surf. Sci. **181**, 295 (1987).
[48]J. S. Hovis, R. J. Hamers, and C. M. Greenlief, Surf. Sci. **440**, L815 (1999).